

Measurement of the $^{234}\text{U}(n,f)$ cross section in the energy range between 14.8 and 17.8 MeV using Micromegas detectors

A. Kalamara^{1,*}, S. Chasapoglou¹, V. Michalopoulou^{1,2}, A. Stamatopoulos¹, Z. Eleme³, M. Kokkoris¹, A. Lagoyannis⁴, N. Patronis³, and R. Vlastou¹

¹Department of Physics, National Technical University of Athens, Zografou campus, 15780 Athens, Greece.

²European Organization of Nuclear Research (CERN), Geneva, Switzerland.

³Department of Physics, University of Ioannina, 45110 Ioannina, Greece.

⁴Tandem Accelerator Laboratory, Institute of Nuclear Physics, N.C.S.R. “Demokritos”, Aghia Paraskevi, 15310 Athens, Greece.

Abstract. The $^{234}\text{U}(n,f)$ reaction cross section was measured for three neutron energies 14.8, 16.5 and 17.8 MeV, relative to the $^{238}\text{U}(n,f)$ reference reaction. The in-beam measurements were carried out by using a set-up based on Micromegas detectors, while the quasi-monoenergetic neutron beams were produced by means of the $^3\text{H}(d,n)^4\text{He}$ reaction at the 5.5MV Tandem T1V25 Accelerator Laboratory of the National Center for Scientific Research “Demokritos” in Athens (Greece). Additionally, α -spectroscopy measurements were performed in order to determine the active mass of the samples and the corresponding impurities. In order to estimate the fission-fragment detection efficiency, Monte Carlo simulations were carried out using the GEF and FLUKA codes. Furthermore, simulations were also performed by coupling the NeuSDesc and MCNP5 codes for the determination of the neutron energy distribution in all the irradiated samples and the results were used in order to correct for the contribution of low energy parasitic neutrons in the fission yield. The final cross section data are presented, along with the methodology adopted for the treatment of the parasitic neutrons.

1 Introduction

Neutron-induced cross sections on actinides are an important element in the design studies for the improvement of nuclear reactors, such as Accelerator Driven Systems (ADS) [1] and Generation-IV reactors (Gen-IV) [2]. These systems are planned to effectively address the important issues of the sustainable use of fuel resources, the proliferation of nuclear material and the transmutation of nuclear waste [3, 4]. Especially, ^{234}U , plays a key role in the Th/U fuel cycle, which is proposed to replace the Pu/U one in advanced nuclear systems.

Various datasets exist in literature for the $^{234}\text{U}(n,f)$ reaction cross section in the energy range from meV to GeV, however, in the energy region between 14–18 MeV, only 7 datasets exist [5–11] that present discrepancies up to 12%, except for the data by Babcock [11], which differ by 60% from the other data. Thus, the purpose of this work is not only to solve the discrepancies in the 14–18 MeV energy region, but also this project is a continuation of two previous ones, published by Stamatopoulos et al. [12] and Tsiniganis et al. [13], in the framework of which the cross section of the $^{234}\text{U}(n,f)$ is measured with quasi-monoenergetic neutrons using the same uranium samples that had been used in the TOF measurements by Karadimos et al. [6]. In Refs. [12, 13], the $^{234}\text{U}(n,f)$ reaction cross section was

measured in the 450–650 keV and 7.5–10 MeV energy regions, implementing the $^7\text{Li}(p,n)$ and the $^2\text{H}(d,n)^3\text{He}$ reactions respectively. In the present work, the results at the 14.8–17.8 MeV region are presented, with the use of the $^3\text{H}(d,n)^4\text{He}$ reaction for the production of the neutron beams.

2 Experimental part

The $^{234}\text{U}(n,f)$ reaction cross section was measured at three energies, namely at 14.5, 16.5 and 17.8 MeV, relative to the $^{238}\text{U}(n,f)$ reference reaction cross section. The three irradiations were carried out at the Tandem T1V25 Accelerator Laboratory of the NCSR “Demokritos”.

The quasi-monoenergetic neutron beams were produced via the $^3\text{H}(d,n)^4\text{He}$ reaction (Q-value=17.59 MeV). More specifically, the deuteron beams were accelerated to energies ranging from 1.8 to 2.8 MeV in order to have sufficient intensities (450–500 nA). Then, they passed through two molybdenum foils of 5 μm thickness each, thus they impinged on the solid Ti-tritiated target with the desirable (lower) energy and therefore, with a higher probability to react with the target atoms, due to the D-T cross section. The flange with the tritium target was air cooled during the irradiations, while the Ti-T target backing was a 1 mm thick Cu foil for good heat conduction. More details on the Ti-T target are given in Refs. [14, 15]. The samples were placed at a distance of ~20 cm from the tritium target, thus limiting their angular acceptance to $\pm 20^\circ$, where the pro-

* Current Address: Institute of Nuclear and Radiological Sciences, Energy, Technology & Safety, N.C.S.R. “Demokritos”, Aghia Paraskevi, 15310 Athens, Greece (email: a.kalamara@ipta.demokritos.gr).

Table 1. Main quantities concerning the irradiations.

Deuteron Energy (MeV)	Neutron Energy (MeV)	Average Current (nA)	Duration (h)	Neutron Fluence ($\times 10^5$ n/cm ² s)
1.8	14.8 \pm 0.3	500	5.0	(2.2 \pm 0.2)
2.3	16.5 \pm 0.3	500	5.5	(4.1 \pm 0.3)
2.8	17.8 \pm 0.2	450	2.7	(1.4 \pm 0.1)

duced neutrons are expected to be practically monoenergetic. The main quantities concerning the irradiations are presented in Table 1.

The ²³⁴U and ²³⁸U samples were produced with the painting technique at the IPPE (Obninsk) and JINR (Dubna). They are thin (~ 5 μ m thick) disks with a 2.6 cm radius deposited on a 100 μ m Al backing [12, 13] and as it was mentioned in Section 1, they are the same samples with those used at the TOF measurements performed at n_TOF by Karadimos et al. [6]. In front of the samples (with respect to the neutron beam) an aluminum mask of 0.6 mm thickness and 2.5 cm radius was placed, so that the desirable angular acceptance was achieved ($\pm 20^\circ$). Furthermore, α -spectroscopy measurements were performed in order to determine the active mass of the samples and the corresponding impurities attributed to the decay of ²³⁴U. A typical spectrum of a ²³⁴U sample is shown in Fig. 1.

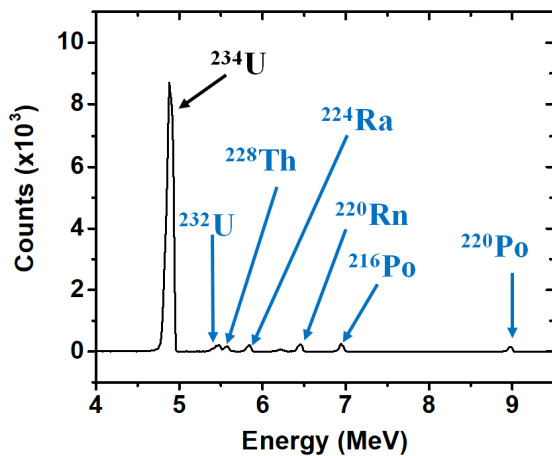


Figure 1. A typical spectrum of α -particles obtained from the ²³⁴U sample. The origin of each α -peak is marked and the impurities were found to be much less than 1% of the total active mass.

In order to perform the in-beam measurements, for each actinide target (²³⁴U, ²³⁸U), a Micromegas detector assembly was used to record the fission fragments. The sample-detector pairs were placed in an Al chamber filled with a Ar:CO₂ (80:20 volume fraction) gas mixture at atmospheric pressure and room temperature, while a more detailed description of the experimental setup is shown in Fig. 2.

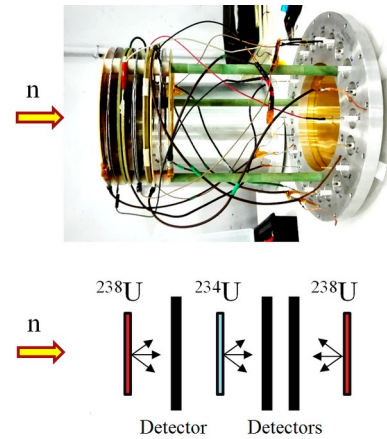


Figure 2. Photograph of the Al chamber interior in which the pairs of sample-detector were placed (top), along with the schematic representation of the target assembly during the irradiation (bottom).

3 Analysis

The cross section was determined according to the following expression:

$$\sigma_{^A U} = \sigma_{^8 U} \cdot \frac{\Phi_{^8 U}}{\Phi_{^A U}} \cdot \frac{N_t^{^8 U}}{N_t^{^A U}} \cdot \frac{N_{ff} \cdot f_{abs} \cdot f_{DT} \cdot f_{cut} \cdot f_{par} \cdot f_{line}^{^A U}}{N_{ff} \cdot f_{abs} \cdot f_{DT} \cdot f_{cut} \cdot f_{par} \cdot f_{line}^{^8 U}} \quad (1)$$

where $\sigma_{^8 U}$ is the reference reaction cross section adopted from the ENDF/B-VIII.0 library [16], Φ is the neutron flux and N_t is the number of the target nuclei. Moreover, N_{ff} is the number of the fission fragments (ff) recorded with the Micromegas detector, while the remaining factors are used to correct this integral (N_{ff}). More specifically, f_{abs} is the absorption of the ff in the samples, f_{DT} is used to correct for the dead-time of the read-out system, f_{cut} is implemented to take into account the rejected ff due to the amplitude threshold introduced in the analysis for the rejection of the α -activity background, while both f_{par} and f_{line} correct for the contribution of low energy parasitic neutrons in the fission yield. The $^A U$ and $^8 U$ subscripts correspond to the ²³⁴U and ²³⁸U samples, respectively.

In order to determine the ratio of the neutron flux in the reference and measured samples ($\Phi_{^8 U}/\Phi_{^A U}$), which is practically the effect of the solid angle in the experimental setup, Monte Carlo simulations were performed by coupling the MCNP5 [17] and the NeuSDec [18] codes. More specifically, the geometry of the irradiation setup was introduced in the MCNP5 code, as shown in Fig. 3, while the neutron source was described by a source definition card (sdef) produced by the NeuSDec code. The shape

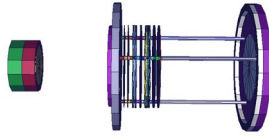


Figure 3. The irradiation setup, as it was described in the MCNP5 simulation (the cap of the chamber is excluded in this figure so that its interior can be seen).

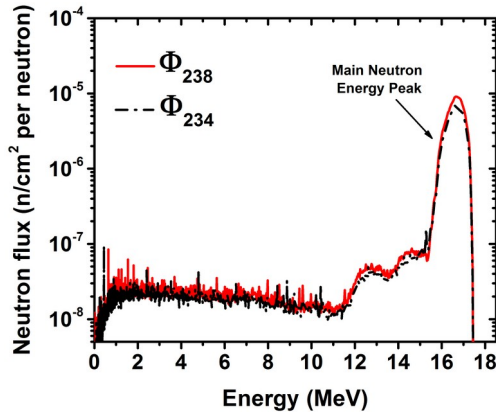


Figure 4. The neutron flux with respect to the neutron energy, as obtained from the MCNP5 simulation for the irradiation at 16.5 MeV neutron energy.

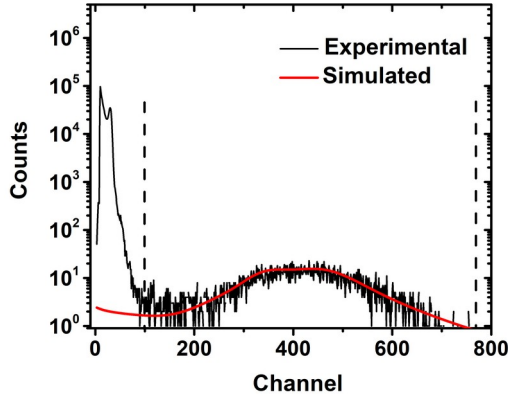


Figure 5. A typical beam-on spectrum obtained with a micro-megas detector (black line), in which the α -background is the peak in the low channel region, while the $\beta\beta$ are those in between the two dashed lines. In addition, the result of the GEF and FLUKA codes convoluted with the response function of the detector is presented, as red line and it was used to determine the f_{cut} .

of the neutron energy distribution, as obtained from the simulation is presented in Fig. 4, while the $\Phi_{^{238}\text{U}}/\Phi_{^{234}\text{U}}$ ratio is determined by the integral of the main neutron energy peak for both ^{234}U and ^{238}U samples. The number of the target nuclei was determined by α -spectroscopy measurements, while the integral of the $\beta\beta$ was determined by the sum of the counts in the region between the two dashed lines in the experimental spectrum shown in Fig. 5. This number ($N_{\beta\beta}$), is then corrected for the dead-time of the

read-out system which was only important for ^{234}U , due to its high α -activity. This correction was implemented through the f_{DT} factor, which was determined by the equation: $f_{DT} = \text{Real Time} / \text{Live Time}$ of the spectrum. Moreover, as it can be seen in Fig. 5, in the low energy region of the experimental spectrum the α -peak (due to the activity of the sample) is present. However, by integrating the region between the two dashed lines in order to reject the α -background, a fraction of $\beta\beta$ is not taken into account. In order to correct for this effect, the mass and energy distributions of the $\beta\beta$ generated from the GEF code [19] were propagated to the detector gas by means of the FLUKA [20, 21] code. The energy deposition in the detector gas was scored and the result of the simulation convoluted with the response function of the detector is shown in Fig. 5, as a red smooth curve. By the aforementioned simulations, the absorption of the $\beta\beta$ in the samples was also estimated and it was found to be less than 2%. Furthermore, the f_{par} factor was determined by the following relation:

$$f_{par} = \frac{RR_{\text{main peak}}}{RR_{\text{total}}} \quad (2)$$

where the RR is the reaction rate, which can be calculated by the following expression:

$$RR = \sum_{E_i} \sigma(E_i) \cdot \Phi(E_i) \quad (3)$$

where σ is the evaluated cross section of the (n,f) reaction of interest, adopted from the ENDF/B-VIII.0 library and Φ is the simulated neutron flux. Last but not least, the f_{fine} factor, which was used to correct for parasitic neutrons that are not taken into account in the simulation (such as (d,n) reactions on materials of the beam pipe) was estimated experimentally. More specifically, each measurement was repeated with the Ti-T target replaced by a Cu foil and eventually, all the recorded $\beta\beta$ attributed to parasitic neutrons from the beam line were estimated by normalizing to the deuteron current of the main beam and were used for the corresponding correction of the fission yields. The values of all the factors of Eq. 1 are given in Table 2.

4 Results and discussion

The $^{234}\text{U}(n,f)$ reaction cross section was measured at three incident neutron energies covering the range between 14.8 and 17.8 MeV and the results are presented in Fig. 6, along with previously existing datasets obtained from EXFOR [22] and the latest evaluations from ENDF/B-VIII.0, JEFF-3.3, JENDL-4.0, CENDL-3.1 and TENDL-2017 libraries [16]. Moreover, the derived cross sections along with their uncertainties are given in Table 3. The cross section uncertainties presented in Fig. 6 and Table 3 correspond to the statistical error of the measurements, while the uncertainties of the N_i for both ^{234}U and ^{238}U (1 and 2%, respectively) are considered systematic. Concerning the uncertainty in the neutron energy, it was determined through the simulation of the irradiation setup, by coupling the NeuSDesc [18] and MCNP5 [17] codes. More specifically, it corresponds to the half of the FWHM of the main neutron energy peak obtained from the simulation.

Table 2. All the quantities of Eq. 1. The first row corresponds to the quantities referred to the irradiation at 14.8 MeV, the second one at 16.5 MeV and the third one at 17.8 MeV. The f_{abs} factor for the ff absorption in the 4U and 8U samples was 2 and 1% , respectively.

$\sigma_{^8U}$ (mb)	$\frac{\Phi_{^8U}}{\Phi_{^4U}}$	4U						8U					
		N_t	N_{ff}	f_{DT}	f_{cut}	f_{par}	f_{line}	N_t	N_{ff}	f_{DT}	f_{cut}	f_{par}	f_{line}
1221	1.29	$4.45 \cdot 10^{18}$	550 ± 23	1.08	1.03	0.87	1.00	$2.12 \cdot 10^{19}$	1933 ± 43	1.00	1.03	0.93	1.00
1318	1.29	$4.45 \cdot 10^{18}$	1241 ± 35	1.08	1.03	0.88	0.99	$2.12 \cdot 10^{19}$	4110 ± 64	1.00	1.03	0.94	0.99
1320	1.29	$4.45 \cdot 10^{18}$	240 ± 16	1.08	1.03	0.84	0.93	$2.12 \cdot 10^{19}$	806 ± 40	1.00	1.03	0.94	0.99

Table 3. Experimental cross section values and uncertainties obtained from the present work for the $^{234}U(n,f)$ reaction.

E_n (MeV)	$\sigma_{^4U}$ (mb)
14.8 ± 0.3	2164 ± 105
16.5 ± 0.3	2489 ± 81
17.8 ± 0.2	2343 ± 172

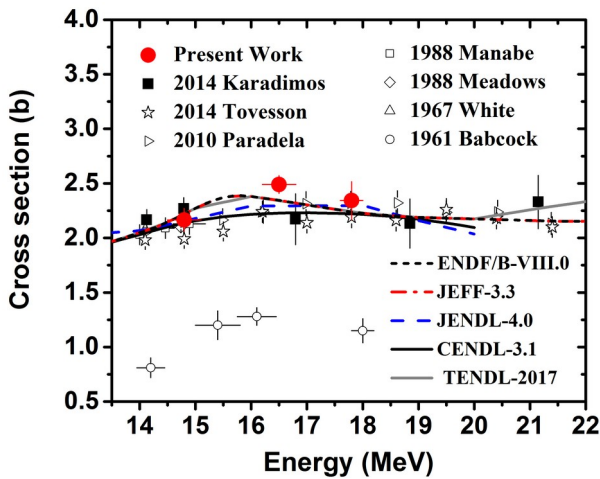


Figure 6. Experimental cross section values of the present work, along with previously existing data points in literature [22] and the ENDF/B-VIII.0, JEFF-3.3, JENDL-4.0, CENDL-3.1 and TENDL-2017 evaluation libraries [16] for the $^{234}U(n,f)$ reaction, in the energy region of interest.

The new experimental data points at 14.8 and 17.8 MeV are in excellent agreement within their errors with previously existing data by Karadimos et al. [6], by Tovesson et al. [5], by Paradela et al. [7], by Manabe et al. [8] and by Meadows [9]. On the contrary, the new data point at 16.5 MeV lies slightly higher than the previously existing data and evaluation libraries. However, it indicates an increasing trend of the cross section curve around 16 MeV, which is also supported by ENDF/B-VIII.0, JEFF-3.3 and TENDL-2017 evaluation curves.

Acknowledgements

The authors would like to acknowledge the assistance of the Accelerator Staff at NCSR “Demokritos”. This research is implemented through IKY scholarships program and co-financed by the European Union (European Social Fund — ESF) and Greek national funds through the action entitled “Reinforcement of Postdoctoral Researchers

- 2nd call (MIS 5033021)”, in the framework of the Operational Programme “Human Resources Development Program, Education and Lifelong Learning” of the National Strategic Reference Framework.

References

- [1] NEA, *Accelerator-driven Systems (ADS) and Fast Reactors (FR) in advanced nuclear fuel Cycles*, Technical Report (Nuclear Energy Agency of the OECD, NEA, 2002).
- [2] <https://www.gen-4.org>, Gen-IV International Forum.
- [3] A. Stanculescu, *Ann. Nucl. Energy* **62**, 607 (2013).
- [4] F. Goldner, R. Versluis, *Transmutation capabilities of Generation 4 Reactors*, Technical Report (Nuclear Energy Agency of the OECD, NEA, 2007).
- [5] F. Tovesson, A. Laptev and T. S. Hill, *Nuclear Science and Engineering*, **178**, 57-65 (2014).
- [6] D. Karadimos and the n_TOF Collaboration, *Phys. Rev. C*, **89**, 044606 (2014).
- [7] C. Paradela and the n_TOF Collaboration, *Phys. Rev. C*, **82**, 034601 (2010).
- [8] Manabe et al., *Technology Reports of the Tohoku University*, **52**, 97-126 (1988).
- [9] J. W. Meadows, *Annals of Nuclear Energy*, **15**, 421-429 (1988).
- [10] P. H. White and G. P. Warner, *Journal of Nuclear Energy*, **21**, 671-679 (1967).
- [11] R. Babcock, Technical Report, Bettis Atomic Power Lab., Westinghouse, Pittsburgh, PA, USA (1961).
- [12] A. Stamatopoulos et al., *Eur. Phys. J. A*, **54**:7 (2018).
- [13] A. Tsinganis et al., using micromegas detectors, *EPJ Web of Conferences*, **146**, 04035 (2017).
- [14] A. Kalamara et al., *Phys. Rev. C*, **93**, 014610 (2016).
- [15] R. Vlastou et al., *Physics Procedia* **66**, 425 (2015).
- [16] ENDF, <https://doi.org/10.1016/j.nds.2011.11.002>
- [17] X-5 Monte Carlo team, Volume I-III, LA-UR-03-1987, LA-CP-03 0245 and LA-CP-03-0284, April (2003).
- [18] E. Birgersson and G. Lovestam, JRC Science Hub Technical Report, Ref. No., 23794, 2009.
- [19] K.H. Schmidt et al., *Nucl. Data Sheets* **131**, 107 (2016).
- [20] A. Ferrari et al., FLUKA: A multi-particle transport code (program version 2005) (CERN, Geneva, 2005) cds.cern.ch/record/898301.
- [21] G. Battistoni et al., *Ann. Nucl. Energy*, **82**, 10 (2015).
- [22] EXFOR, <http://www.nndc.bnl.gov/exfor/exfor.htm>